Proceedings of ISAP'04, Sendai, JAPAN

1C2-2

ESTIMATION OF ELECTRIC PARAMETERS OF METALS AND LIQUIDS FROM THE KNOWLEDGE OF THE PROPAGATION EFFECT THROUGH THE MATERIAL

Toshihide Tosaka Isamu Nagano Satoshi Yagitani
Graduate school of Natural Science and Technology, Kanazawa University
2-40-20 Kodatsuno, Kanazawa-shi, Ishikawa 920-8667, Japan
tosaka@reg.is.t.kanazawa-u.ac.jp

1. Introduction

With the continuing development of information and electrical technology, the number and kinds of electric devices in our society have increased rapidly. It has been shown that electromagnetic waves leaking from electronic devices may cause incorrect operation of other electronic devices. One method to eliminate the electromagnetic noise which is emitted from electric devices is the use of an electromagnetic shielding sheet. In order to eliminate the electromagnetic noise, the design of the electromagnetic shielding sheet must take into account the electromagnetic field from various noise source points. To do this properly, we must investigate the propagation mechanism of the electromagnetic wave by using numerical analysis. Then it is important to know the electric parameters (ε_r, μ_r, σ), because they determine the attenuation of an electromagnetic wave. However, many electromagnetic shielding sheets are covered by metal plating. The resulting uneven surface makes it difficult to estimate the electric parameters.

In this research, we used a shield box in order to easily measure the Shielding Effectiveness (*SE*). We estimate the electric parameters by considering the propagation of waves through metallic materials and liquid materials. For the numerical calculations, we had to consider the location of the source, and we used the Sommerfeld integral that expresses spherical waves by compositions of cylindrical waves [1]. We fitted the calculated values to measurement values, and we were able to estimate the electric parameters. We then evaluated our method by comparing the values obtained by our method with the nominal values [2].

2. Measurement of shielding effectiveness for the electric field and for the magnetic field

In this research, we used two types of shield boxes. One, which we designed, is used to measure the *SE* for the magnetic field. The other shield box, TR17301A developed by Advantest corporation, is commercially available and is used to measure the *SE* for the electric field. A transmitter and a receiver are located in these shield boxes. The planes of the transmitting and receiving loop antennas and the testing materials are parallel in both shield boxes.

The *SE* of the magnetic field (SE_H) is expressed by eq. (1). The SE_H is defined as the ratio of the magnetic field strength at the receiver without the testing material (H_0) to that with the testing material (H_1). The *SE* of the electric field (SE_E) is expressed by eq. (2). The SE_E is similarly defined as the ratio of the electric field strength at the receiver without the testing material (E_0) to that with the testing material (E_1). For the measurement SE_E of liquid materials, we used a container made of acrylic that has no influence on SE_E .

$$SE_H = 20\log_{10}\frac{|H_0|}{|H_1|} \qquad (1) \qquad\qquad SE_E = 20\log_{10}\frac{|E_0|}{|E_1|} \qquad (2)$$

3. Calculations of the electromagnetic field

In calculating an electromagnetic field, we have to consider the locations of the source and the observation point, because the calculations of an electromagnetic field for a near-field point and that for a distant point are quite different. If the distance z from the observation point to a source with wave length λ is $z \gg \lambda/2\pi$, the radiated field is the dominant wave emitted from the source and can be regarded as a plane wave. In this case, the *SE* of the shielding material is not related to the position of the source. But in the shield boxes we used, the distance of the source from the observation point is z

ISBN: 4-88552-206-4 C3055©IEICE

≪λ/2π, and it can not be considered that the radiated field is the wave emitted from source. Thus it is necessary to calculate the electromagnetic field of a near source when calculating *SE*. In this research in consideration of the near source, we used the Sommerfeld integral that expresses spherical waves by a composition of cylindrical waves.

4. The calculation model and boundary conditions

Our calculation model is the Multi-layered model shown in fig. 1. The source is assumed to be at $z=h$ with homogenous layers above and below the dipole extending to infinity in the horizontal directions. The axial direction of the dipole source is located vertically perpendicular to each layer. Π_i expresses the Hertz vector in the *i*th layer. The superscript *u* identifies the up-going wave; *d* is the down-going wave, and *p* is the direct wave.

The electromagnetic field emitted from an electric dipole is expressed by eq. (3) and eq. (4) using the Hertz vector Π expressed in Eq. (5). When a loop antenna is used to simulate a magnetic dipole, the electromagnetic field is expressed by eq. (6) and eq. (7) using a magnetic Hertz vector Π_m expressed in Eq. (8). For the magnetic Hertz vector, the second subscript, the one following the *m*, identifies the layer.

$$H = j\omega\varepsilon\nabla\times\Pi \quad (3) \qquad E = -j\omega\mu\nabla\times\Pi_m \quad (6)$$

$$E = \nabla\nabla\cdot\Pi + k^2\Pi \quad (4) \qquad H = \nabla\nabla\cdot\Pi_m + k^2\Pi_m \quad (7)$$

$$\Pi = \frac{Il}{j4\pi\omega\varepsilon}\frac{e^{-jkR}}{R}i_z \quad (5) \qquad \Pi_m = \frac{nSI}{4\pi}\frac{e^{-jkR}}{R}i_z \quad (8)$$

In these equations, *E* is the electric field; *H* is the magnetic field; *ω* is the angular frequency; *ε* is the dielectric constant; *μ* is the relative permeability; *k* is the wave number; *l* is the length of the electric probe antennas; *n* is the number of turns of wire on the loop antenna; *S* is the loop area; *I* is the current, and *R* is the distance from the source.

The boundary conditions between the layers *i* and *i*+1 on the *x-y* plane are given in eqs. (9), (10), (11), and (12). Eq. (9) and (10) are the boundary conditions for the electric field, and eq. (11) and (12) are the boundary conditions for the magnetic field.

$$\frac{\partial\Pi_i}{\partial z} = \frac{\partial\Pi_{i+1}}{\partial z} \quad (9) \qquad \frac{\partial\Pi_{m,i}}{\partial z} = \frac{\partial\Pi_{m,i+1}}{\partial z} \quad (11)$$

$$\varepsilon_i\Pi_i = \varepsilon_{i+1}\Pi_{i+1} \quad (10) \qquad \mu_i\Pi_{m,i} = \mu_{i+1}\Pi_{m,i+1} \quad (12)$$

The Hertz vectors for layer *i* are expressed in eq. (13) and (16) as the sum of an up-going wave and a down-going wave for the electric and magnetic fields, respectively. By using the Sommerfeld integral representation to express a spherical wave as a synthesis of cylindrical waves, the Hertz vectors expressed in eq. (5) and (8) can be transformed into eq. (14) and (17) for the up-going waves and into eq. (15) and (18) for the down-going waves, respectively, for layer *i*

$$\Pi_i = \Pi_i^u + \Pi_i^d \quad (13) \qquad \Pi_{m,i} = \Pi_{m,i}^u + \Pi_{m,i}^d \quad (16)$$

$$\Pi_i^u = \frac{Il}{j4\pi\omega\varepsilon}\int_0^\infty f_i^u(\lambda)J_0(\lambda r)e^{-\upsilon_i(z-z_i)}\lambda d\lambda \quad (14) \qquad \Pi_{m,i}^u = \frac{nSI}{4\pi}\int_0^\infty f_{m,i}^u(\lambda)J_0(\lambda r)e^{-\upsilon_i(z-z_i)}\lambda d\lambda \quad (17)$$

$$\Pi_i^d = \frac{Il}{j4\pi\omega\varepsilon}\int_0^\infty f_i^d(\lambda)J_0(\lambda r)e^{\upsilon_i(z-z_i)}\lambda d\lambda \quad (15) \qquad \Pi_{m,i}^d = \frac{nSI}{4\pi}\int_0^\infty f_{m,i}^d(\lambda)J_0(\lambda r)e^{\upsilon_i(z-z_i)}\lambda d\lambda \quad (18)$$

$$\text{Here} \quad \upsilon_i = \sqrt{\lambda^2 - k_i^2}$$

The integral elements $f_i(\lambda)$ and $f_{m,i}(\lambda)$ are unknown functions of the integration variable *λ* with the subscripts and superscripts the same as for the respective Hertz vectors; J_0 is a zero-order Bessel function of the first kind; *r* is the radial distance in cylindrical coordinates, and z_i is the distance of layer *i* along the *z*-axis.

5. Estimation of electric parameters

In order to estimate the electric parameters, we first measured *SE* with the shield box. Then from these *SE*, we estimate the electric parameters of metallic materials and liquid materials. The *SE* calculations are most influenced by the electric parameters. *SE* has different characteristics as a function of frequency for different types of materials. Fig. 2 shows SE_H of metal materials, and Fig. 3 shows SE_E of liquid materials. In the case of diamagnetic materials (Al, Pb, Cu) and liquid materials, the measurement value and the calculation value that used the nominal value of the electric parameters are very close. In these cases, we can estimate the electric parameters with high accuracy. But for ferromagnetic materials, as the frequency becomes high, the calculated *SE* becomes much larger than the measured *SE*.

Therefore, we then calculated *SE* by taking the frequency characteristics into account. Fig. 4 shows *SE* when the frequency characteristics of the relative permeability were considered. From fig. 2 in the low frequency region where the calculated and measured *SE* values were close, we used the estimation method to determine the conductivity which does not change with frequency. Using the conductivity as a constant, we then varied the relative permeability to find the minimum value of the difference. In this computation, we used the least squares method.

In this way, by changing the relative permeability parameter, we can estimate the frequency characteristics of the relative permeability as shown in Fig. 5. Since most of the data of relative permeability available in reference books are for DC, we have to determine for ourselves the nominal values for the AC case. In order to determine the nominal values for the AC case, we determined the relative permeability as a function of frequency by using B-H curves generators. When this was completed, we evaluated our estimation method.

6. Results of estimations

Table 1 shows the relative permeability and conductivity of metal materials. The calculated conductivity was the same as the nominal value for Pb, 1.9% greater for Cu, and 3.3% greater for Al. For the ferromagnetic materials, the calculated value was 4.1% higher for Ni and 9.8% higher for Fe. For comparison, measurement of conductivity using four point probe method had a typical error rate of about 20%. Thus, we find that our method is better than the existing method. The nominal values for the relative permeability of the ferromagnetic materials are close to the values derived with our B-H curve testing as shown in Fig. 5. For Fe, the nominal and calculated ranged from the same to 3% difference. For Ni, they ranged from the same to 33% difference from the nominal values.

Table 2 shows the dielectric constant of liquid materials. The calculated dielectric constant was the same as the nominal value for Glycerin, 1.2% smaller for pure water, and 2.0% greater for physiological saline (1.2wt% NaCl). The values of the conductivity of the liquid materials are very small. Most of the conductivities of liquid materials are less than 2 *S/m*. These values are very small and we can ignore them. The most important parameters of SE_E are the dielectric constants which determine the SE_E curve. Therefore, we did not estimate the conductivity of the liquid materials.

7. Conclusion

We measured SE_E and SE_H using a shield box. Since near-field and far-field calculation methods are different, we had to consider the distance from the source to the observation point. For our measurements, the distances from the dipole source to the observation point are smaller than a wave length. We calculated the electromagnetic field at the observation point by using the Sommerfeld integral that expresses spherical waves as compositions of cylindrical waves.

Measurement values of the diamagnetic materials and the liquid materials of *SE* are very close to the calculated *SE* values using nominal electric parameters, and we were able to estimate the electric parameters easily. But in the case of ferromagnetic materials, the measurement values and the calculated values differ as the frequency increases. When we considered the frequency characteristics of the electric parameters, changing the parameters allowed us to determine the relative permeability and conductivity as a function of frequency.

Using our method, we can estimate the electric parameters not only for diamagnetic materials and liquid materials but also for ferromagnetic materials. This will be very useful for the design of electromagnetic shielding sheets.

8. Reference

[1] I. Nagano, Y. Yoshimura, S. Yagitani, H. Yokomoto, T. Tosaka, and T. Nakayabu, "Estimation of

Electric Parameters of Thin Electromagnetic Shielding Materials, ” *IEE trans. Fm*, Vol.123, No. 2, pp. 192–199, Feb. 2003.
[2] F. M. Tesche, M. V. Ianoz, T. Karlsson, “EMC analysis methods and computational models, ” *A Wiley-Interscience*, pp. 550–552, 1997.

9. Figures and tables

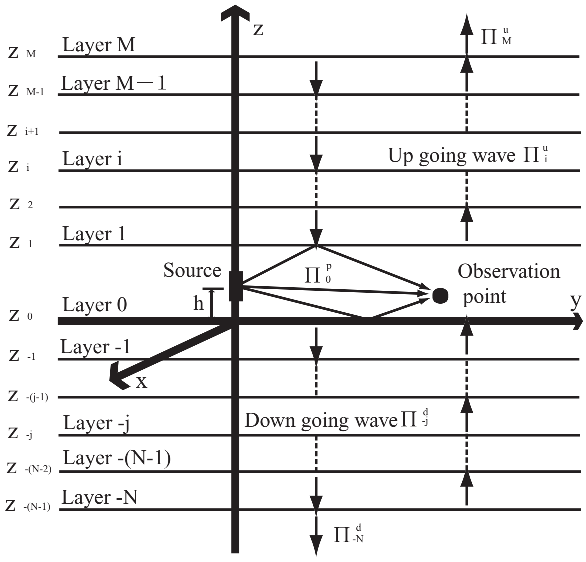

Fig. 1. Multi-layered model

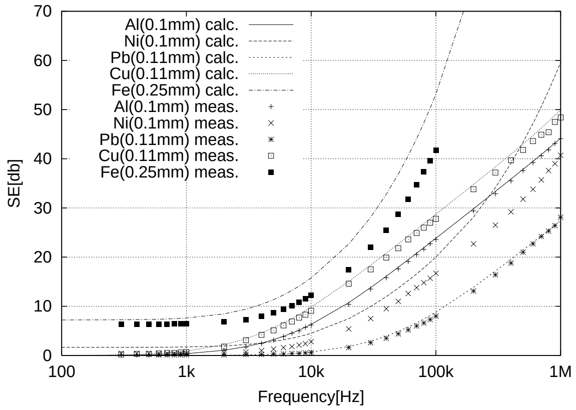

Fig. 2. *SE* of metallic materials

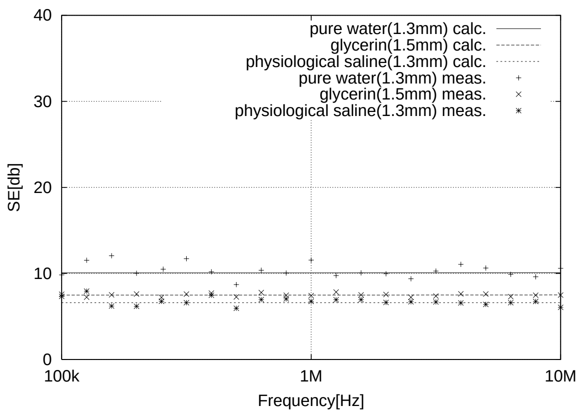

Fig. 3. *SE* of liquid materials

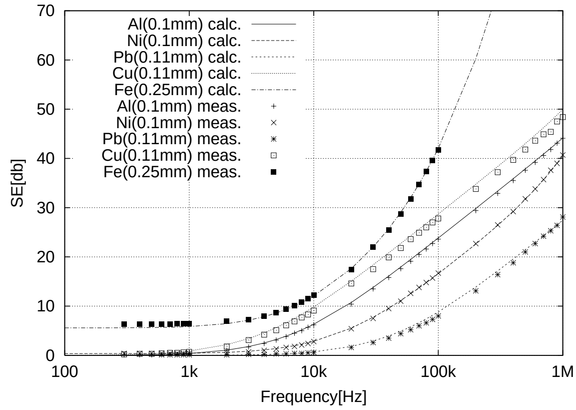

Fig. 4. *SE* of metallic materials after consideration of frequency characteristics

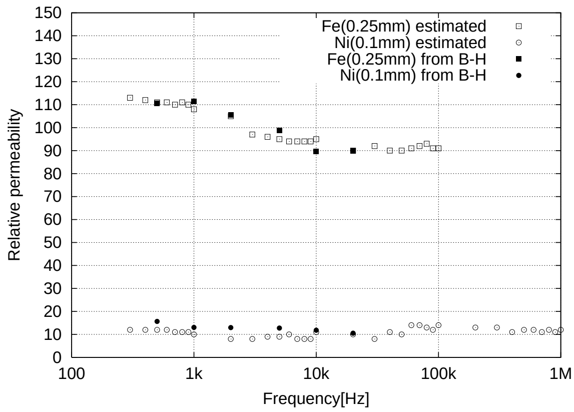

Fig. 5. The frequency characteristics of the relative permeability

Table 1. Relative permeability and conductivity of metal materials

Materials (thickness)	μ_r [nom. / calc.]	σ [nom. / calc.] [S/m]
Al (0.1mm)	1.0 / 1.0	3.63×10^7 / 3.51×10^7
Cu (0.11mm)	1.0 / 1.0	5.80×10^7 / 5.69×10^7
Pb (0.11mm)	1.0 / 1.0	0.50×10^7 / 0.50×10^7
Fe (0.25mm)	111.0 / 108.0	1.02×10^7 / 0.92×10^7
Ni (0.1mm)	13.0 / 10.0	1.45×10^7 / 1.39×10^7

Relative permeability of Fe and Ni are at 1kHz

Table 2. Dielectric constant of liquid materials

Materials (thickness)	ε_r [nom. / calc.]
Pure Water (1.3mm)	81.0 / 80.0
Glycerin (1.5mm)	50.0 / 50.0
Physiological saline (1.3mm)	49.0 / 50.0